National Aeronautics and Space Administration

Orbital Debris
Quarterly News

Volume 12, Issue 1

January 2008
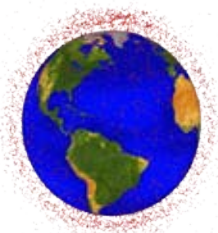
A publication of

The NASA Orbital Debris Program Office

Two Minor Fragmentations End Worst Debris Year Ever

After witnessing the worst satellite breakup in history on 11 January, the year 2007 ended on a much quieter note with only two minor events recorded during the fourth quarter. The two fragmentations occurred only a day apart in early November and fortunately, should have little effect on the long-term, near-Earth environment.

In 2005, the highly successful, 14-year mission of NASA's Upper Atmosphere Research Satellite (UARS) came to an end with final maneuvers to place the spacecraft into a short-lived, disposal orbit and the implementation of passivation measures (ODQN, January 2006, pp. 1-2). For the next two years, UARS (International Designator 1991-063B,

U.S. Satellite Number 21701) gradually lost altitude, coming closer to its eventual fiery reentry (Figure 1). However, on 10 November 2007, at least four debris were unexpectedly ejected from the 5.7-metric-ton spacecraft with moderate velocities.

Two debris (U.S. Satellite Numbers 32291 and 32292) were thrown in a retrograde direction, while the other two debris (U.S. Satellite Numbers 32297 and 32298) were sent on posigrade trajectories. One fragment was found in an orbit with a period more than one minute less than that of UARS, whereas the period of another fragment gained two minutes. Initially, a few other debris were thought to have been
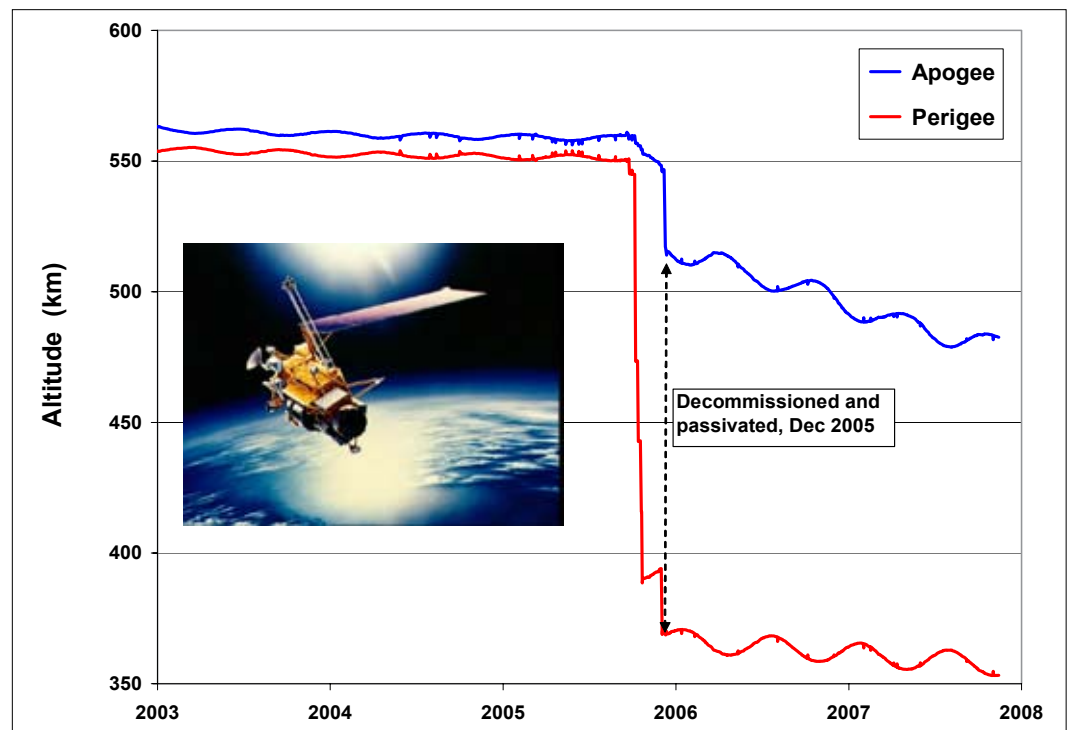
Figure 1. UARS decayed naturally for 2 years after its end of mission before experiencing a minor fragmentation event.

Two Minor Fragmentations

continued from page 1

detected by the U.S. Space Surveillance Network, but they could not be found with follow-up observations. The two lower orbital debris fell back to Earth by the end of November, leaving only two debris remaining in orbit at the end of the year.

The cause of UARS' minor fragmentation is still under investigation. The spacecraft had been purged of all propellants and its batteries had been left in a safed state. Only a slight amount of pressurant is judged to have been a potential energy source at the time of the event. The UARS structure appears to be essentially unchanged with no significant change in its orbital decay rate. One explanation for this anomalous event is a strike by a small, untracked particle, although the exact cause is likely to remain unknown.

The day after the incident with UARS, the U.S. conducted the first Delta IV launch vehicle mission of 2007. The previous flight had taken place in November 2006 and had resulted in the unplanned release of more than 60 debris shortly after orbital injection of the second stage (ODQN, January 2007, p. 2). Due to their release altitude near 850 km, only five of the debris had fallen out of orbit a year later. Despite an intense investigative effort, the source of the debris, which did not affect the subsequent workings of the stage, could not be identified with high confidence. Hence, the flight of USA 197 on 11 November 2007 was of particular interest to space surveillance and orbital debris specialists.

This latest flight of the Delta IV launch vehicle called for the second stage to achieve three distinct orbits: a low-Earth parking orbit, a geosynchronous transfer orbit, and a nearly geosynchronous payload delivery orbit. Like its predecessor, this second stage (International Designator 2007-054B, U.S. Satellite Number 32288) also produced large (>10 cm) debris after entering Earth orbit. At least two dozen debris appear to have been released after the stage reached its temporary parking orbit, which was reported to be approximately 220 km by 1575 km (Figure 2).

Also, like the 2006 mission, the debris released had no apparent detrimental effect on the performance of the stage which successfully carried its payload to the planned destination orbit. An investigation into the source mechanism for the debris continues.

Overall, 10 fragmentation events were identified during 2007, including the now infamous deliberate breakup of the Fengyun-1C spacecraft by the People's Republic of China and the accidental, but very serious, explosion of the Russian Arabsat 4 Briz-M orbital stage. The increase in cataloged orbital debris was by far the most of any year of the space age, and the consequences will be felt for many, many years to come. ◆
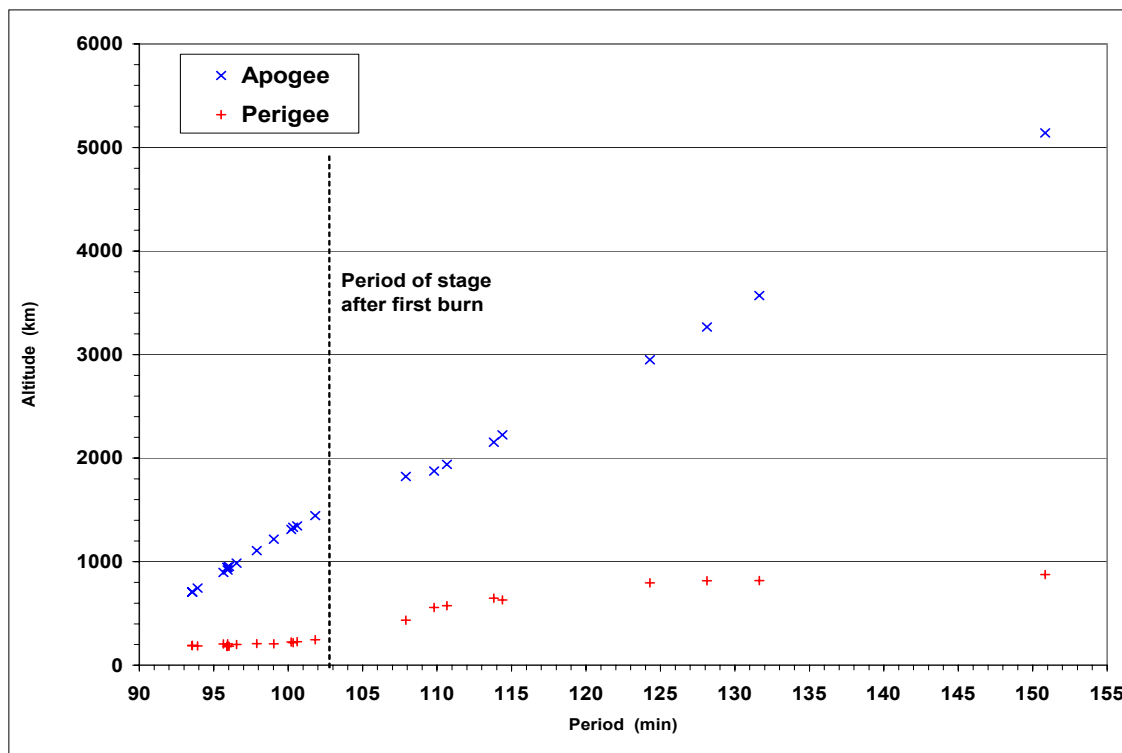
Figure 2. Two dozen debris from the USA 197 Delta IV second stage were identified soon after launch.

Fengyun-1C Debris: One Year Later

Although quickly recognized as the worst satellite breakup in history, the true magnitude of the deliberate destruction of the Fengyun-1C spacecraft is only now coming into sharper focus. The U.S. Space Surveillance Network (SSN) continues to identify new, large debris in low Earth orbit (LEO), while special observations by the Haystack radar provide insight into the much larger numbers of smaller, potentially hazardous orbital debris.

The 8-year-old, nearly one-metric-ton Fengyun-1C spacecraft was used as a target on 11 January 2007 for the test of an anti-satellite (ASAT) system by the People's Republic of China (ODQN, April 2007, pp. 2-3). Impacted by a direct-ascent interceptor at a speed of approximately 9 km/s at an altitude near 850 km, the spacecraft disintegrated, spreading debris throughout LEO and beyond.

By the end of the year, the SSN had officially cataloged 2317 debris, of which only 22 (less than 1%) had reentered the atmosphere. Figure 1 compares the catalog populations in January 2007 and January 2008.

Debris
continued from page 2

More than 250 additional debris had been tentatively identified with Fengyun-1C and were being tracked by the SSN, bringing the total large debris (most larger than 10 cm) count to nearly 2600. Figure 2 indicates that China is responsible for nearly half of all known and tracked satellite breakup debris currently in Earth orbit.

Meanwhile, observations of the Fengyun-1C debris cloud by the higher frequency Haystack (X-band) radar permit characterization of debris as small as 5 mm. Data analysis by NASA's Orbital Debris Program personnel suggests that the total number of Fengyun-1C orbital debris one centimeter and larger was at least 150,000. Consequently, both the large

and small Fengyun-1C debris populations are now assessed to considerably exceed model predictions. Since NASA's breakup model is empirically based upon both terrestrial and in-orbit hypervelocity impact tests, the reason for Fengyun-1C's more prolific nature is under investigation. ♦
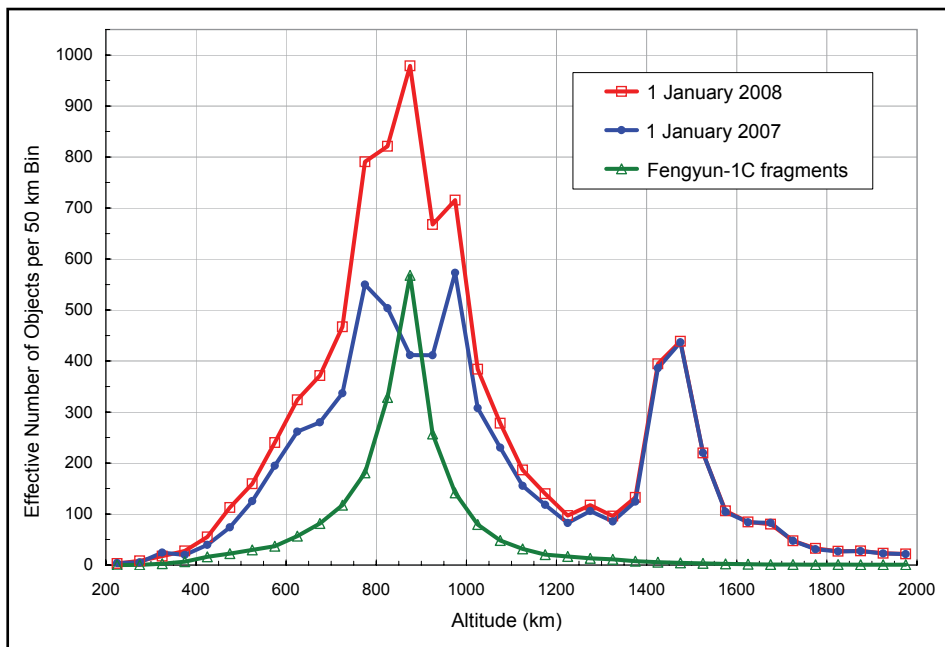
Figure 1. Distributions of the catalog populations in the low Earth orbit region in January 2007 (blue), January 2008 (red), and the officially cataloged Fengyun-1C fragments.
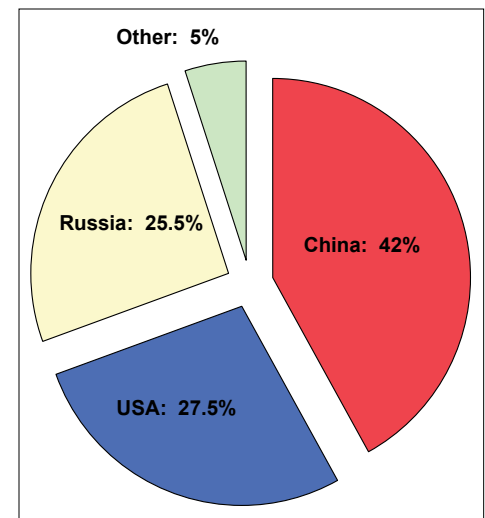
Figure 2. The People's Republic of China was responsible for nearly half of all known satellite breakup debris in orbit as of 1 January 2008. The primary source of this debris was the intentional destruction of the Fengyun-1C spacecraft.

PROJECT REVIEWS

STS-118 Radiator Impact Damage

D. LEAR, J. HYDE, E. CHRISTIANSEN, J. HERRIN, AND F. LYONS

During the August 2007 STS-118 mission to the International Space Station, a micrometeoroid or orbital debris (MMOD) particle impacted and completely penetrated one of shuttle Endeavour's radiator panels and the underlying thermal control system (TCS) blanket, leaving deposits on (but no damage to) the payload bay door. While it is not unusual for shuttle orbiters to be impacted by small MMOD particles, the damage from this impact is larger than any previously seen on the shuttle radiator panels.

A close-up photograph of the impact entry hole is shown in Figure 1, and the location of the impact on Endeavour's left-side, aft-most

radiator panel is shown in Figure 2. The aft radiator panel is 12.7 mm (0.5 inch) thick and consists of 0.28 mm (0.011 inch) thick aluminum facesheets on the front and back of an aluminum honeycomb core. In addition, the front facesheet is covered by a 0.13 mm (0.005 inch) thick layer of silver Teflon thermal tape. The entry hole in the silver Teflon tape measured 8.1 mm by 6.4 mm (0.32 inch by 0.25 inch). The entry hole in the outer facesheet measured 7.4 mm by 5.3 mm (0.29 inch by 0.21 inch). The impactor also perforated an existing 0.3 mm (0.012 inch) doubler that had been bonded over the facesheet to repair previous impact damage (an example that
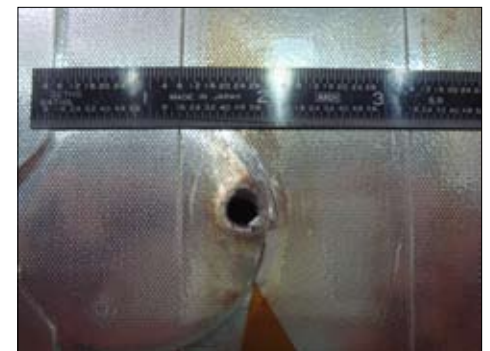
Figure 1. Entry-hole damage to Endeavour's left-side aft-most radiator panel observed during post-flight inspection.

3

STS-118

continued from page 3
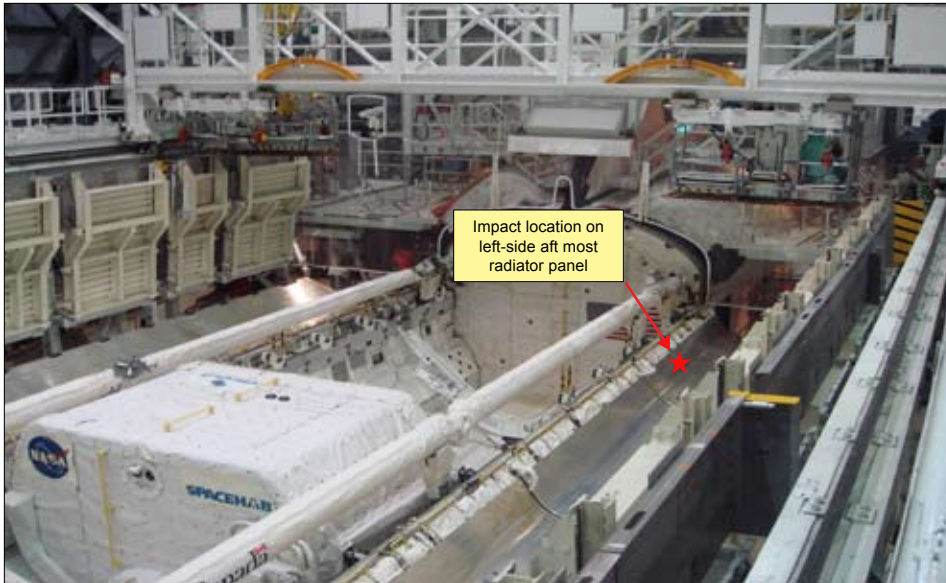
Figure 2. Impact damage location on Endeavour's left-side radiator panel # 4 (LH4).

Figure 3. Exit hole in the rear facesheet of the radiator panel.

Figure 4. Damage to thermal control system blanket (two impact locations).
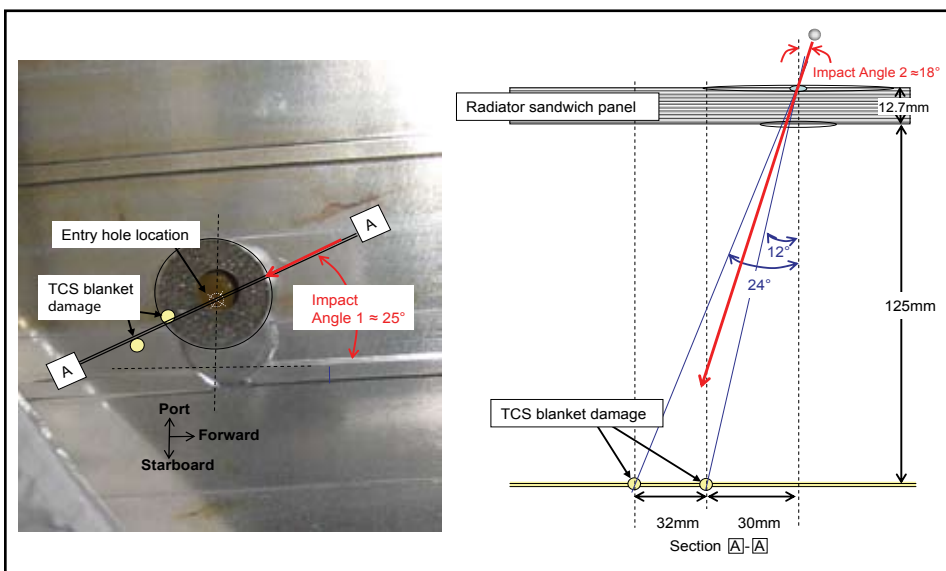
Figure 5. Estimated orientation of MMOD impactor.

lightning can strike the same place twice, even for MMOD impact). The peeled-back edge around the entry hole, or "lip," is a characteristic of many hypervelocity impacts. Hypervelocity impact with the front facesheet fragmented the impacting particle and caused it to spread out into a debris cloud. The debris cloud caused considerable damage to the internal honeycomb core, with 23 honeycomb cells over a region of 28 mm by 26 mm (1.1 inch by 1.0 inch) having either been completely destroyed or partially damaged. Figure 3 is a view of the exit hole in the rear facesheet that partially shows the extent of the honeycomb core damage and clearly shows the jagged, "petaled" exit hole through the backside facesheet. The rear facesheet's exit hole damage, including cracks in the facesheet, measures 14 mm by 14 mm (0.55 inch by 0.55 inch). The remnants of the impacting particle and radiator panel material blown through the rear facesheet hole also created two penetrations in the TCS blanket 125 mm (4.9 inches) behind the rear facesheet. Figure 4 shows these two impacts, which are located 32 mm (1.25 inches) apart. Some deposits of material were found on the payload bay door beneath the TCS blanket, but no additional damage occurred to the door.

Figure 5 illustrates the relationship of the facesheet entry hole to the TCS blanket damage, which may indicate the direction of the impacting particle. The image on the left side of Figure 5 shows an overhead view of the damaged radiator after the facesheet holes were cored out of the panel. The entry hole location and the two underlying TCS blanket damage sites are annotated on the image. Section A-A, running through the entry hole and TCS blanket damage locations, describes a 25° angle from the longitudinal axis of the shuttle. The second impact angle can be seen in section A-A on the right side of Figure 5. An average 18° angle of impact to the surface normal was derived by measuring the angles of the two damage sites in the TCS blanket to the entry hole.

As part of the radiator repair procedure, intact core samples were collected of the outer thermal tape, outer facesheet, honeycomb core, and rear facesheet. Swabs of the two impact damage areas on the TCS blanket were also collected. Micrometeoroid and orbital debris impacts usually leave residual particulates from the impactor material in and around the damaged area. This residue is collected, analyzed, and in many cases, a determination can be made as to

STS-118
continued from page 4

the impactor source being micrometeoroid or orbital debris. In some cases, specific types of orbital debris particles can be identified, such as rocket propellant or electrical components. To perform this analysis, the samples were transferred to the NASA Johnson Space Center Hypervelocity Impact Technology Facility in Houston, Texas. Scanning Electron Microscopes (SEM) equipped with Energy-Dispersive X-ray (EDX) Spectrometry tools will identify potential residue material from the impactor and the elemental makeup of the impactor. Early results from this analysis indicate that the impacting particle was a titanium-rich orbital debris particle containing traces of zinc and possibly antimony.

Additionally, hypervelocity impact tests are being conducted at the NASA White Sands Test Facility on realistic, simulated radiator panel material in order to duplicate the observed damage. The impacting particle size will be estimated using information from field data and SEM analysis on particle density, impact velocity, and impact angle. Early impact test results suggest that the particle size was approximately 1.5 mm to 2.0 mm in diameter, assuming that the particle was orbital debris. Final results of the SEM/EDX analysis and the hypervelocity impact tests will be described in a post-flight MMOD damage report. ♦

Debris Assessment Software 2.0 Now Available

J. OPIELA AND N. JOHNSON

NASA's Debris Assessment Software (DAS) has been totally redesigned and rebuilt. With the release of the new NASA Technical Standard 8719.14, "Process for Limiting Orbital Debris," the new DAS 2.0 is now available for public distribution. DAS is designed to assist NASA programs in performing orbital debris assessments, as described in the Standard. As in previous versions, the software follows the structure of the Standard and provides the user with tools to assess compliance with the requirements. If a project is non-compliant, DAS may also be used to explore debris mitigation options to bring the project within the requirements.

The release of DAS 2.0 includes a new, native Microsoft Windows graphical user interface (GUI), which is a vast improvement over the old DOS-based interface. The new software also includes on-line help features familiar to Windows users. The user will enter detailed information about each of their launched objects into the "Mission Editor" (Figure 1). Launched objects include payloads, rocket bodies, and mission-related debris. Data entered in the Mission Editor describe the operational and post-mission orbits of the launched objects. The data are then available to the various assessment modules, without having to be reentered. The entire project may also be saved for later reference or re-use.

After filling in the Mission Editor, the user will select "Requirement Assessments". This brings up another "dialog" window listing the Requirements assessed within DAS. These include: mission-related debris crossing low Earth orbit (LEO) and passing through or near the geosynchronous (GEO) region, intentional breakups, probability of collision with large and small debris, post-mission disposal, reentry survivability, and hazards of space tether systems. Most assessments allow the user to review the input data and mouse-click a "Run" button to begin assessment. Some modules (collisions, reentry survivability, and tethers) require the user to enter additional information before proceeding with the assessment. For ease of use, the entered information may be saved and reloaded from "csv" (comma-separated values) text files.

In addition to the assessment modules, the user will still have a number of "Science and Engineering" modules to assist in the assessment process. These modules help the user determine the probability of on-orbit collisions, analyze post-mission disposal options, predict orbital evolution, estimate an object's cross-sectional area, and perform other minor calculations related to DAS. The Science and Engineering section also includes a stand-alone version of the reentry survivability module, disconnected from the assessment process. This module requires additional inputs, but allows the user to explore more options without changing the input characteristics of the actual mission.

Underlying routines within the DAS code have also been improved. DAS 2.0 includes updated models for propagation, the debris environment, and reentry survivability. The "fast" propagator used by the previous DAS (version 1.5.3) is replaced by NASA's newer propagators, "PROP3D" and "GEOPROP". These are the propagators used by NASA's debris evolutionary models. Although they take longer to run, the new propagators produce more accurate results. Improved force models include Earth's atmosphere and gravitational field, solar and lunar gravitation, and solar radiation pressure. The solar flux value (used for atmospheric drag calculations) is no longer a user input; the user will now enter the date, and the appropriate values will
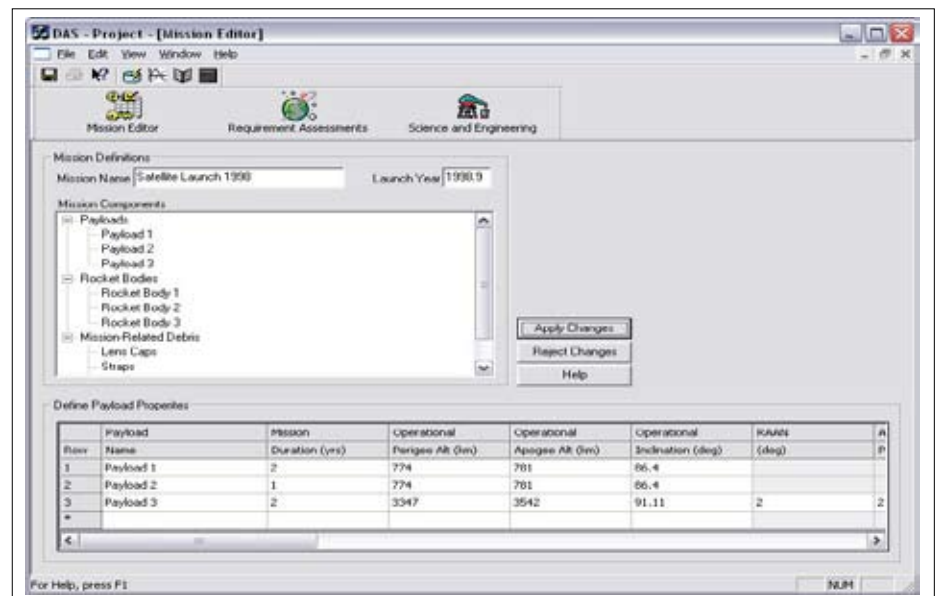
Figure 1. DAS 2.0 Mission Editor.

DAS 2.0

continued from page 5

be retrieved from a model based on standard data published by the National Oceanic and Atmospheric Administration (NOAA). The future projection of solar activity is a repeating cycle, computed as the curve fit to all daily historical values (ODQN, April 2006, pp. 4-5). The debris environment has been updated from the previous ORDEM96 model to the newer ORDEM2000 (ODQN, April 2002, p. 1). Inclusion of these improvements and updates is the greatest contributor to the increased size of the DAS software package.

Numerous upgrades have been applied to the assessment of human casualty due to reentering debris. Routines based on NASA's Object Reentry Survival Analysis Tool (ORSAT version 6) determine which objects might survive reentry, and the resulting risk of casualty is calculated based on an updated world population database. Improvements in the reentry routines include the specification of orbital inclination, an improved aero-heating model, temperature-dependant material properties (for the included materials), and improved impact kinetic energy calculation. Up to 200 unique hardware components may now be entered in up to four nested levels. This last feature allows the software to more accurately model components which are exposed below the initial breakup altitude.

DAS 2.0 includes a new plot viewer and a new materials database. The plot viewer (Figure 2) allows the user to modify the plot properties (titles, labels, axis limits, line

colors, etc.). Plots may be copied directly to the Windows "clipboard," then pasted into documents or image editors. As mentioned above, the improved materials database includes temperature-dependant specific heat for the many included materials. The user may also enter new materials into a project-specific list of user-defined materials. This will allow an infinite variety of materials, including mixed materials. Unlike the included materials, the user-defined materials will have fixed properties

(no temperature dependence).

As NASA's standard method of assessing compliance with the new NS 8719.14, the new DAS 2.0 will be an important tool for use in space mission design. The many improvements in the interface and the underlying models have yielded a product that is both higher fidelity and easier to use than previous versions of DAS. For more information about DAS 2.0, please visit the NASA Orbital Debris Program Office website. ♦
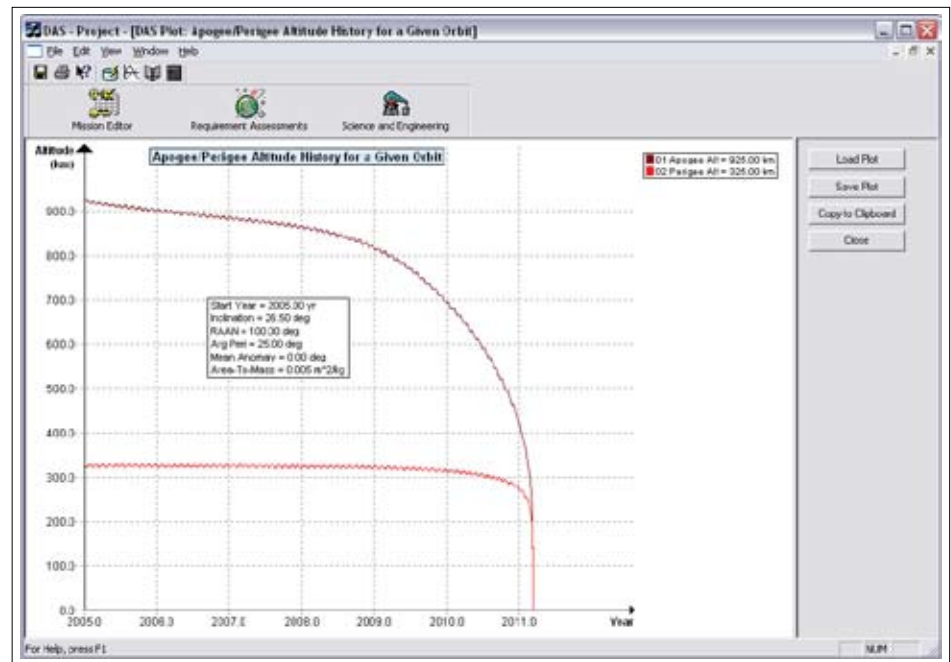
Figure 2. DAS 2.0 Orbit Evolution Analysis.

Seasonal Variations of the MODEST Data

H. RODRIGUEZ, K. ABERCROMBY, E. BARKER, M. MATNEY, M. MULROONEY, AND P. SEITZER

The Michigan Orbital DEbris Survey Telescope (MODEST), a 0.6/0.9-m Schmidt telescope located at the Cerro Tololo Inter-American Observatory (CTIO) in Chile, has been collecting data for the NASA Orbital Debris Program Office since 2002.[1] Once the observational data are processed and analyzed, the resultant data are correlated with the tracked satellite catalog maintained by the U.S. Space Surveillance Network (SSN). Objects not in the catalog are defined as uncorrelated targets (UCTs). Our Orbital Debris Program Office is attempting to gain a better understanding of the physical characteristics of orbital debris by studying known correlated targets. Using

the optical brightness variations of correlated targets, we can derive a model to predict light curve behavior as a function of target shape. This model will lead to determining the size and shape of orbital debris, whose photometric behavior is similar to non-functional correlated targets.

Correlated objects can be categorized by the shape and functionality of the object in relation to phase angle (sun-object-observer angle), solar declination, and day of year (DOY). The major shape categories are defined as box and cylinder; other cases will be addressed in the future to include more complex shapes comparable to orbital debris. The functionality of a target is determined by whether it is still performing station-keeping maneuvers at the time of the observation. By studying correlated

targets (CTs) where the size and shape of the objects are known, a shape distribution of compared brightness can be defined. These results will lead to defining a UCT shape distribution and eventually a more accurate size estimation. Currently, an estimate of size is determined by using the object's magnitude and assuming a diffuse Lambertian sphere.[2] This model is not applicable for all targets for it does not take into account orientation or shape. The following seasonal variation results include correlated targets as starting points in determining size, shape, and orientation effects on brightness in an attempt to interpret orbital debris light curves. The objects discussed in this article were observed by MODEST a minimum

MODEST

of 15 times between January of 2002 and March of 2007.

The study of seasonal variations is complex due to multiple attributes that can affect an object's magnitude. A functional satellite will show brightness variations as a function of its geometry and viewing angles (*i.e.,* boxes will show greater brightness variations, or glints, than cylinders at specular viewing angles because of the greater cross section).[2, 3] When comparing the target's brightness with DOY, it is important to note the selection effects (*i.e.,* observations are limited to when the sky is photometric). Some objects were seen twice in one night (both trailing and leading the anti solar-point), with absolute magnitude variations as high as three orders of magnitude, which is primarily due to the orientation of the target at that particular point in the orbit. This analysis explores how the absolute magnitude of an object is dependent on the shape, functionality, DOY, and solar declination. The normalized absolute magnitude is used for this article since it has been range- and phase-angle- corrected using a diffuse Lambertian sphere model. Since the phase angle dependence was removed for all the data, any variation in brightness is a deviation from the Lambertian assumption and/or real variations due to shape, orientation, or surface type. The broad R (560-740 nm) magnitudes vary within each observational period, but those variations and phase angle dependence will be studied in future research.[4] The absolute magnitude data in this article are the average of all the broad R magnitudes obtained during a typical observing window (typically 5 minutes long or eight independent detections), which are then normalized by the target's first measured brightness in the survey period covered by this paper.

Thirty-four targets, in total, were investigated and categorized by bus type (shape) and functionality. Boxes, defined as cube-like/rectangular shapes with two solar panels and usually with two parabolic reflectors, make up approximately 85% of the targets. Of this percentage, 79% are functional (F) boxes and 21% are non-functional (NF) boxes (three of the six non-functional boxes became non-functional during the observation time). Cylinders, all of which are functional, are simply cylindrical- or drum-shaped and make up 15% of the total.

The first shape category analyzed was the functional box-type targets. Common to this subset were brightness peaks between DOY (82 to 112) and DOY 261, corresponding to

solar declination angles between 1.18º to 12.2º and 1.96º, respectively; previous studies have shown solar declination dependence for similar satellite shapes.[2] The first peak occurs close to the fall equinox for the southern hemisphere and the second peak near the spring equinox. Between late April and mid-September (DOY 113 to 260) no data were analyzed due to the criteria for 15 or more observations as well as lack of scheduled observation time. Some of the functional targets did have secondary minor variations in brightness at a different DOY as well, which could be due to the orientation of the target and material dependence (specular or diffuse reflections) of the target. One target with behavior contrary to this trend is seen in Figure 1; two boxes (yellow and green) are the same bus type, approximately the same size, and both are body stabilized, but have different trends in magnitude. One reason for this difference could be observing geometry. In general, the functional boxes show a two-peak signature in absolute magnitude.

The non-functional boxes, on the other hand, did not show a trend, but rather a random spread over the observing days (shown with triangles and boxes in Figure 2). The nonfunctional boxes showed a decrease in magnitude (darkening) by an order of two or more magnitudes over time compared to their functional state. Only one nonfunctional box (red arrow points to one data point: black

triangle with pink outline) did not display the same magnitude decrease because the date on which it became inactive was very recent and it often takes several months before an obvious change in magnitude is detected (presumably due to the object's tumbling). Data were collected on three non-functional cylinders (all non-functional prior to observing run) as well, but were only observed 10 to 14 times. The variations in absolute magnitude are similar to non-functional boxes, having a comparably constant magnitude across all solar declinations (or DOY), with random peaks due to specular or diffuse reflections. The cylinders are shown in Figure 2 and can be located by the triangles that are yellow, orange, and green with blue outlines.

Functional cylinders were also studied to evaluate any trends or peaks in brightness over the observing time. The results are shown in Figure 3. Since there are fewer observed cylindrical bus types, it is difficult to make a firm conclusion, but a similar brightness variation trend as that of active boxes can be seen with some of the targets. All of the cylinders were spin-stabilized, unlike the boxes that are 3-axis stabilized. DOY 91 and 261 mark the two prominent peaks (DOY 91 being the most dominant), correlating with solar declinations of 4.7º and 1.96º. These peaks also correspond with the southern hemisphere's autumnal and
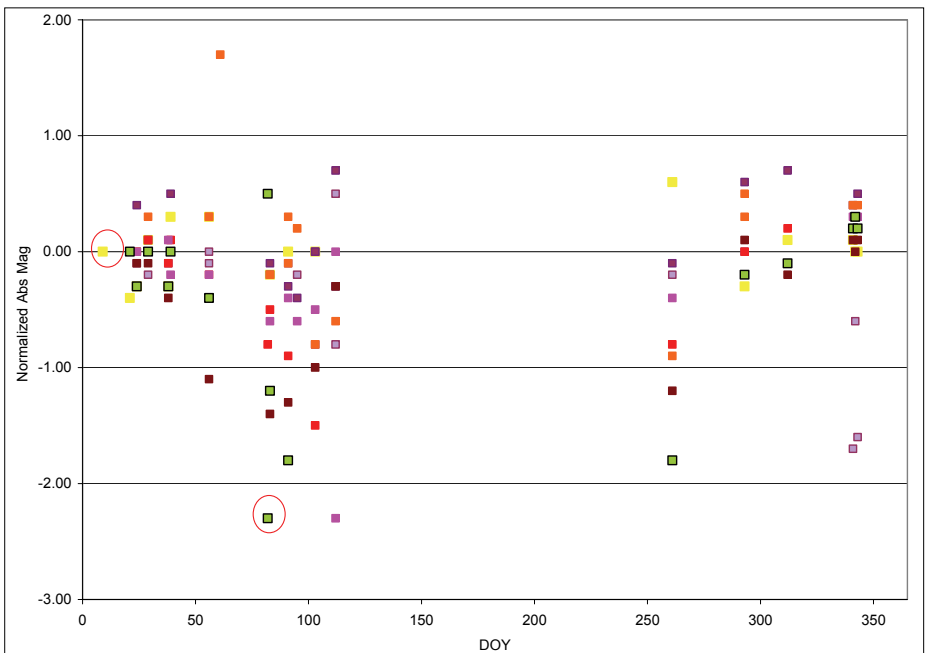
Figure 1. Plot of boxes as a function of normalized absolute magnitude and DOY. Each color represents an individual target.

MODEST

continued from page 7

vernal equinox. With more data, it is possible the cylinders will show at least one other brightness peak similar to the data with cylindrical shapes on the CCD Debris Telescope (CDT).[2]

From the data discussed here, it is apparent that shapes and functionality (*e.g.*, orientation) significantly affect light curves. Data for cylinders were limited, but show a similar trend in brightness to boxes (but at somewhat different and multiple solar declinations). A comparison between boxes and cylinders shows that boxes generally tend to be slightly brighter except at the cylinder peaks in solar declination (DOY 92 and 261), similar to the results with the CDT data.[2] The non-functional boxes are the only targets that simulate the diffuse Lambertian approximation, keeping relatively constant absolute magnitude over all seasons (all DOY and solar declinations). We can conclude from this study that non-functional targets and not station-kept objects should be used in our attempt to model debris light curves and that non-functional targets show the closest light curves to orbital debris, since debris are believed to be tumbling and likely are not simple shapes. Additional research is currently being conducted on how non-functional cylinders compare with functional cylinders, as well as non-functional boxes. The box and tumbling cylinder data sets show systematic variations with seasons, indicating that their photometric behavior is more like a flat plate with a fixed orientation than a sphere. With thirty-four objects total, statistically acceptable conclusions on seasonal variations would require more data on the cylinder types as well as an increased number of detections acquired through MODEST.

Future work will further investigate these variations and attempt to derive an alternate model to explain the positive correlation between brightness and the equinoxes. We also intend to investigate the variation in broadband R magnitude for each observational period and perform a rigorous statistical evaluation of the brightness variations, specifically the difference in the standard deviations between boxes, cylinders, and other shapes. In an effort to develop a shape distribution relative to the optical brightness for the targets, more complex shapes will be presented, which will give further insight into the orbital debris environment at GEO. ♦

1. Seitzer, P., et al. *"A Survey for Space Debris on Geosynchronous Orbit,"* 2001 AMOS Technical Conference Proceedings, Kihei, Maui, HI, 2002.

2. Jarvis, K., et al. *Changes Seen in Three Years of Photometry for GEO Objects*, IAC-03-IAA.5.1.05, 54th International Astronautical Congress, Bremen, Germany, 2003.

3. Lambert, J., et al. *"Observed Optical Brightness Distributions of Deep Space Satellites,"* 2002 AMOS Technical Conference Proceedings, Kihei, Maui, HI, 2002.

4. Payne, T., et al. *"Satellite Monitoring, Change Detection, and Characterization Using Non-Resolved Electro-Optical Data From a Small Aperture Telescope,"* 2007 AMOS Technical Conference Proceedings, Kihei, Maui, HI, 2007.
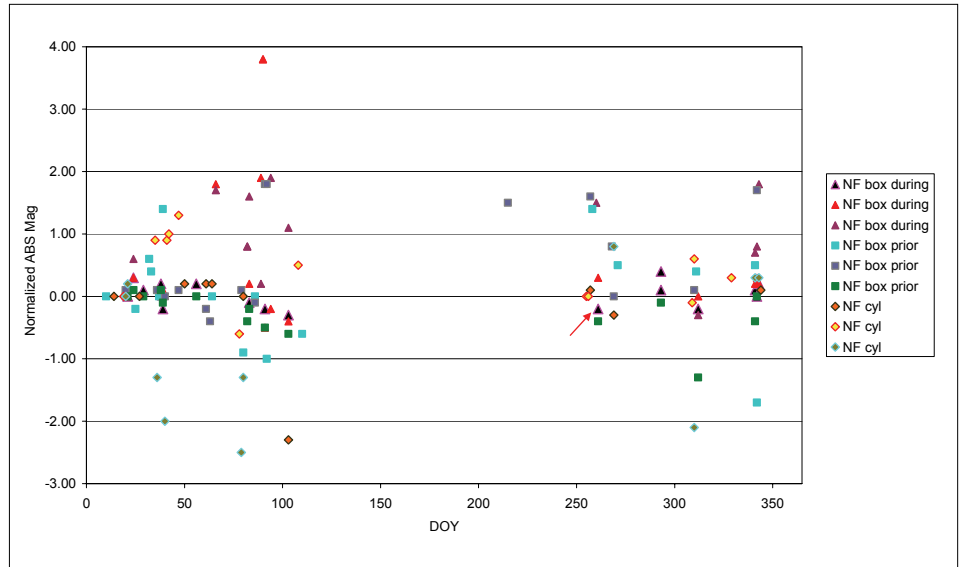
Figure 2. Nonfunctional targets, normalized absolute magnitude vs. DOY – '▲' NF box during observation run, '■' NF box prior to observation run, '◊' all NF cylinders prior to observation run. Each color represents an individual target.
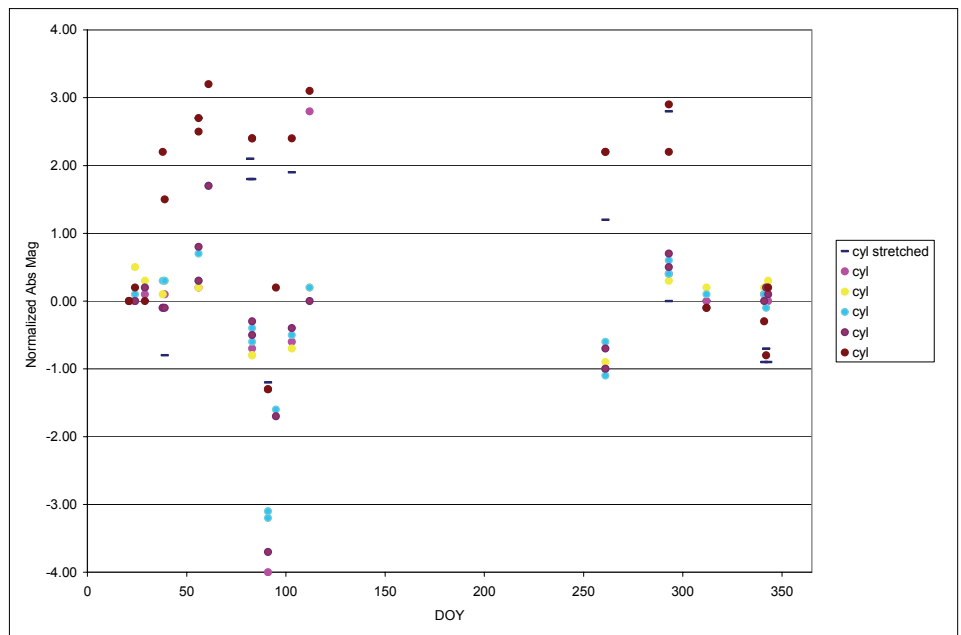
Figure 3. Cylinders plotted normalized absolute magnitude vs. DOY. Each color represents an individual target.

Measurement of Satellite Impact Fragments

N. HILL AND A. STEVENS

The characterization of breakup fragmentation debris has evolved in the last decade from the consideration of debris as spheres toward that of describing debris in terms of size, material, and shape parameters. Fragments and photographs are available from a number of hypervelocity impact ground tests. Specifically, results are analyzed from: Satellite Orbital Debris Characterization Impact Test – SOCIT3 and SOCIT4;[1] European Space Operations Centre ground tests;[2] the XonTech test of the NASA Size Estimation Model – SEM;[3] and Kyushu University tests.[4] These data have contributed to the overall goal of the NASA Orbital Debris Program Office to provide reliable measurements of these parameters.

The NASA Orbital Debris Program Office uses characteristic length as the standard for defining the size of an object. Accurate measurements of characteristic length have been difficult in a few past cases due to irregular shapes of debris and confusion by analysts regarding the definition of this size parameter.

Characteristic length is defined as:

$$L_C = \frac{X + Y + Z}{3}$$

where X, Y, and Z are the maximum orthogonal projections of the object shadow. Characteristic length defines the object's size as it would be portrayed in space – tumbling, averaged over those longest dimensions. For example, the characteristic length of a sphere is its diameter.

Measurement techniques, such as suspending an object by wires, manipulating the object by hand, and setting the object on graph paper, have in the past affected the interpretation of X, Y, and Z. All require determination of dimensions based solely upon visual judgment. Currently, no systematic methods are in use to determine the uncertainty of calculations based on these measurement techniques.[5]

With the common goal of mitigating these inaccuracies, allaying any misunderstandings, and of moving forward in fragment shape determination, the NASA Orbital Debris Program Office began an investigation into the use of a computerized measurement system in early 2007. A handheld laser scanner, the HandyScan3D®, was chosen for the task. The scanner uses two cameras to triangulate the position of the object of study against a reference board. The user manually scans the entire surface of the object, thereby generating
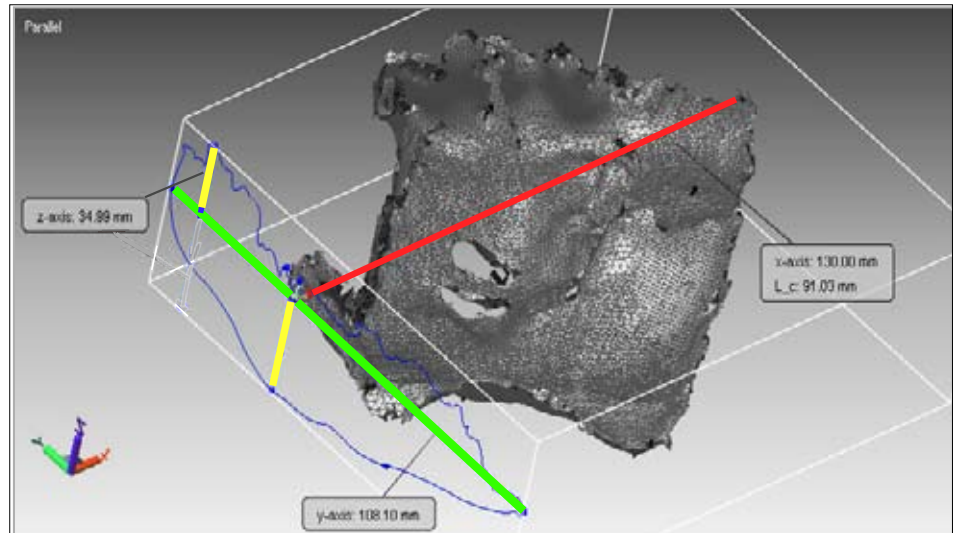
Figure 1. Display of SOCIT4 fragment showing X (red), Y (green), and Z (yellow) and the shadow outline in the Y-Z plane.

a representative cloud of points that is stored in the system software.

Further analysis is performed in a more advanced software package, RapidForm®, which transforms the point cloud to a three-dimensional surface within a Cartesian coordinate system and allows assignment of dimensions. Figure 1 displays an example of a SOCIT4 fragment as it was analyzed for this
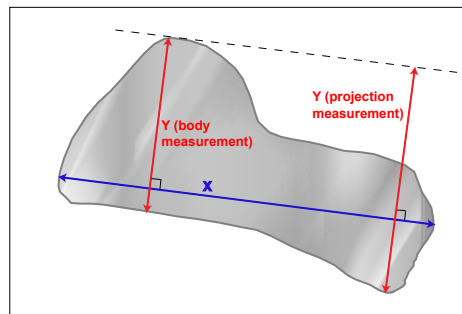
Figure 2. A 2-D picture of X and Y dimensions – portraying body and projection measurements.

investigation. The X dimension was identified as the longest shadow dimension of the object. The plane perpendicular to X contains the shadow that defines Y and Z.

By convention, Y is defined as the longest shadow dimension, or projection measurement, perpendicular to X (Figure 2). Note that the body measurement is the longest perpendicular dimension along the body, whereas the projection measurement is the longest perpendicular dimension along the shadow.

By similar convention, Z is the longest overall projection orthogonal to both X and Y (Figure 3). The projection of Z is the sum of two separate measurements.

To date, ten SOCIT4 fragments have been scanned and had three-dimensional images stored for future shape analysis. As shown in Table 1, the results from the computerized method are compared to the measurements made by hand-manipulation. As expected, the

Table 1. Comparison of handheld and computerized measurements.

	Handheld Measurements (cm)				HandyScan3D® Measurements (cm)			
	X	Y	Z	Lc	X	Y	Z	Lc
1	13.0	10.6	3.0	8.9	13.0	10.8	3.5	9.1
2	16.2	5.6	3.3	8.4	16.5	5.7	3.2	8.5
3	11.0	3.9	2.0	5.6	11.0	3.9	2.3	5.7
4	29.6	8.7	5.0	14.4	29.3	7.7	5.8	14.3
5	10.5	10.5	2.9	8.0	10.6	9.7	2.5	7.6
6	19.1	6.8	1.2	9.0	18.9	6.6	1.2	8.9
7	8.1	7.3	3.9	6.4	8.0	6.8	4.0	6.2
8	9.7	7.0	0.7	5.8	10.1	7.3	1.1	6.2

Measurement

continued from page 9

X dimension is the most consistent between the two methods because the longest overall dimension is the easiest to identify using either technique. The measurement in the Y dimension differs slightly, but the main discrepancy is in the Z dimension. This results in a revision to characteristic length. Importantly, these measurements can be difficult to acquire using hand-manipulation of the target, but the computerized technique is straightforward, repeatable, and the resulting measurement error is negligible.

Measurement documentation will always include at least one digital picture of the object in its scanning position taken by a standard camera. In addition, there will be at least one JPEG image of the object that clearly labels each axis and gives the characteristic length (see Figure 1). Finally, there will be a live image with which the user can rotate the object in three dimensions to view all sides from multiple perspectives.

Additional uses of this computerized method may include area analyses. This technology can also measure the cross-sectional and surface areas of an object, which is useful in Lc-to-area and area-to-mass analysis. As dimension and shape measurements improve in accuracy, there will be a corresponding improvement in the interpretation of optical and radar measurements of the orbital debris population.

The NASA Orbital Program Office has adopted a new technique for characterizing break-up fragments. The new scanning procedure always includes using the projection method for every dimension of the object. As a result, the technology NASA is using makes measurement results more accurate than prior methods, and provides complete documentation and repeatability for future shape analysis. ♦

1. Reynolds, et al. *NASA Standard Breakup Model 1998 Revision*, 1998.

2. Fucke, W., Sdunnus, H. *Population Model of Small Size Space Debris,* ESOC Contract No. 9266/90/D/MD, 1993.

3. Settecerri, T., Stansbery, E., Hebert, T. *Radar Measurements of the Orbital Debris Environment: Haystack and HAX Radars October 1990 through October 1998,* JSC-28744, 1999.

4. Hanada, T., Sakuraba, K., Liou J.-C. *Three New Satellite Impact Tests,* ODQN, Vol. 11 Issue 4, p. 4, 2007.

5. Madler, R.A. *A New Analysis on the Size Estimation Model Pieces*, ODQN, Vol. 11 Issue 1, p. 4, 2007.
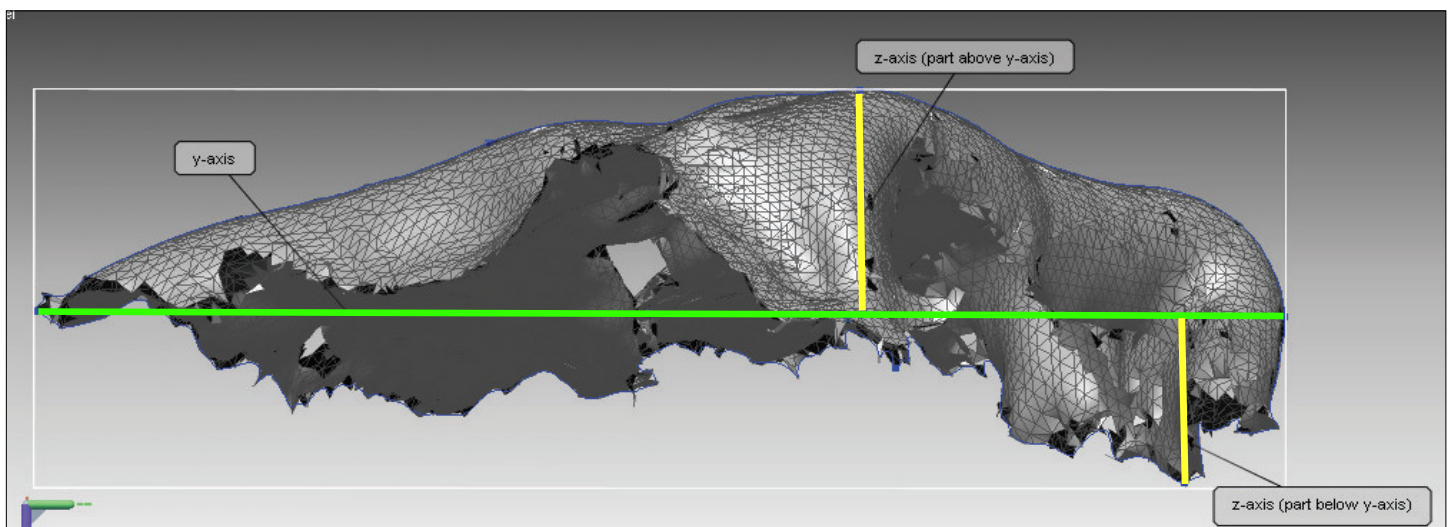
Figure 3. The projection of Z is the sum of two separate measurements.

UPCOMING MEETINGS

13 - 20 July 2008: The 37th COSPAR Scientific Assembly, Montréal, Canada.

Three debris sessions are planned for the conference. They will address advances in ground-based and in-situ measurement techniques; debris and meteoroid environment models and related collision risk estimates for space missions; on-orbit collision avoidance; re-entry risk assessments; debris mitigation measures and their effectiveness for long-term environment stability; national and international debris mitigation standards and guidelines; hypervelocity impact technologies; and on-orbit shielding concepts. The abstract submission deadline is 17 February 2008. Additional information for the conference is available at <http://www.cospar2008.org/index.html>.

29 September - 3 October, 2008: The 59th International Astronautical Congress, Glasgow, Scotland.

A Space Debris Symposium is planned for the 2008 IAC. Five sessions are scheduled for the Symposium to address various technical issues of space debris, including measurements, modeling, risk assessments, reentry, hypervelocity impacts, protection, mitigation, and standards. The abstract submission deadline is 11 March 2008. Additional information about the symposium is available at <http://www.iac2008.co.uk/>.

INTERNATIONAL SPACE MISSIONS
01 October – 02 January 2008

International Designator	Payloads	Country/ Organization	Perigee (KM)	Apogee (KM)	Inclination (DEG)	Earth Orbital Rocket Bodies	Other Cataloged Debris
2007-044A	OPTUS D2	AUSTRALIA	35775	35798	0.1	1	1
2007-044B	INTELSAT 11 (PAS 11)	INTELSAT	35776	35798	0.0		
2007-045A	SOYUZ-TMA 11	RUSSIA	334	337	51.6	1	0
2007-046A	WGS F1 (USA 195)	USA	35786	35787	0.0	1	0
2007-047A	NAVSTAR 60 (USA 196)	USA	20151	20212	54.9	2	0
2007-048A	GLOBALSTAR M067	USA	918	936	52.0	1	0
2007-048B	GLOBALSTAR M070	USA	1413	1415	52.0		
2007-048C	GLOBALSTAR M066	USA	915	936	52.0		
2007-048D	GLOBALSTAR M068	USA	913	938	52.0		
2007-049A	COSMOS 2430	RUSSIA	492	39848	63.0	2	2
2007-050A	STS 120	USA	234	339	51.6	0	0
2007-051A	CHANG'E 1	CHINA	LUNAR ORBIT			1	0
2007-052A	COSMOS 2433 (GLONASS)	RUSSIA	19129	19130	64.9	2	2
2007-052B	COSMOS 2432 (GLONASS)	RUSSIA	19092	19168	64.9		
2007-052C	COSMOS 2431 (GLONASS)	RUSSIA	19085	19175	64.9		
2007-053A	SAR LUPE 3	GERMANY	475	495	98.2	1	0
2007-054A	USA 197	USA	NO ELEMS. AVAILABLE			1	0
2007-055A	YAOGAN 3	CHINA	627	630	97.8	1	0
2007-056A	STAR ONE C1	BRAZIL	35777	35797	0.0	1	1
2007-056B	SKYNET 5B	UK	35595	35709	0.1		
2007-057A	SES SIRIUS 4	SWEDEN	35741	35747	0.0	1	1
2007-058A	COSMOS 2434	RUSSIA	35778	35797	0.1	1	1
2007-059A	SKYMED 2	ITALY	622	624	97.9	1	0
2007-060A	USA 198	USA	NO ELEMS. AVAILABLE			1	0
2007-061A	RADARSAT 2	CANADA	792	799	98.6	1	0
2007-062A	NAVSTAR 61 (USA 199)	USA	20144	20317	55.0	2	0
2007-063A	RASCOM 1	RASCOM	EN ROUTE TO GEO			1	1
2007-063B	HORIZONS 2	INTELSAT	EN ROUTE TO GEO				
2007-064A	PROGRESS-M 62	RUSSIA	334	337	51.6	1	0
2007-065A	COSMOS 2435 (GLONASS)	RUSSIA	19142	19378	64.7	2	2
2007-065B	COSMOS 2436 (GLONASS)	RUSSIA	18982	19126	64.7		
2007-065C	COSMOS 2437 (GLONASS)	RUSSIA	19148	19367	64.7		

ORBITAL BOX SCORE
(as of 02 JAN 2008, as cataloged by the U.S. SPACE SURVEILLANCE NETWORK)

Country/ Organization	Payloads	Rocket Bodies & Debris	Total
CHINA	63	2634	2697
CIS	1369	2951	4320
ESA	37	36	73
FRANCE	47	321	368
INDIA	34	106	140
JAPAN	102	69	171
US	1081	3119	4200
OTHER	396	91	487
TOTAL	3129	9327	12456

Technical Editor
J.-C. Liou

Managing Editor
Debi Shoots

Correspondence concerning the ODQN can be sent to:
Debi Shoots
NASA Johnson Space Center
Orbital Debris Program Office
Mail Code JE104
Houston, TX 77058

debra.d.shoots@nasa.gov

Monthly Number of Objects in Earth Orbit by Object Type

Total

Fragmentation Debris

Spacecraft

Rocket Bodies

Mission-related Debris

Number of Objects

Year
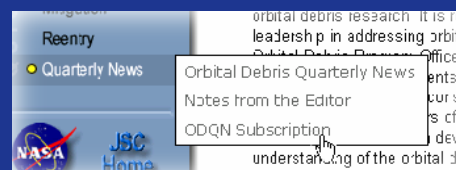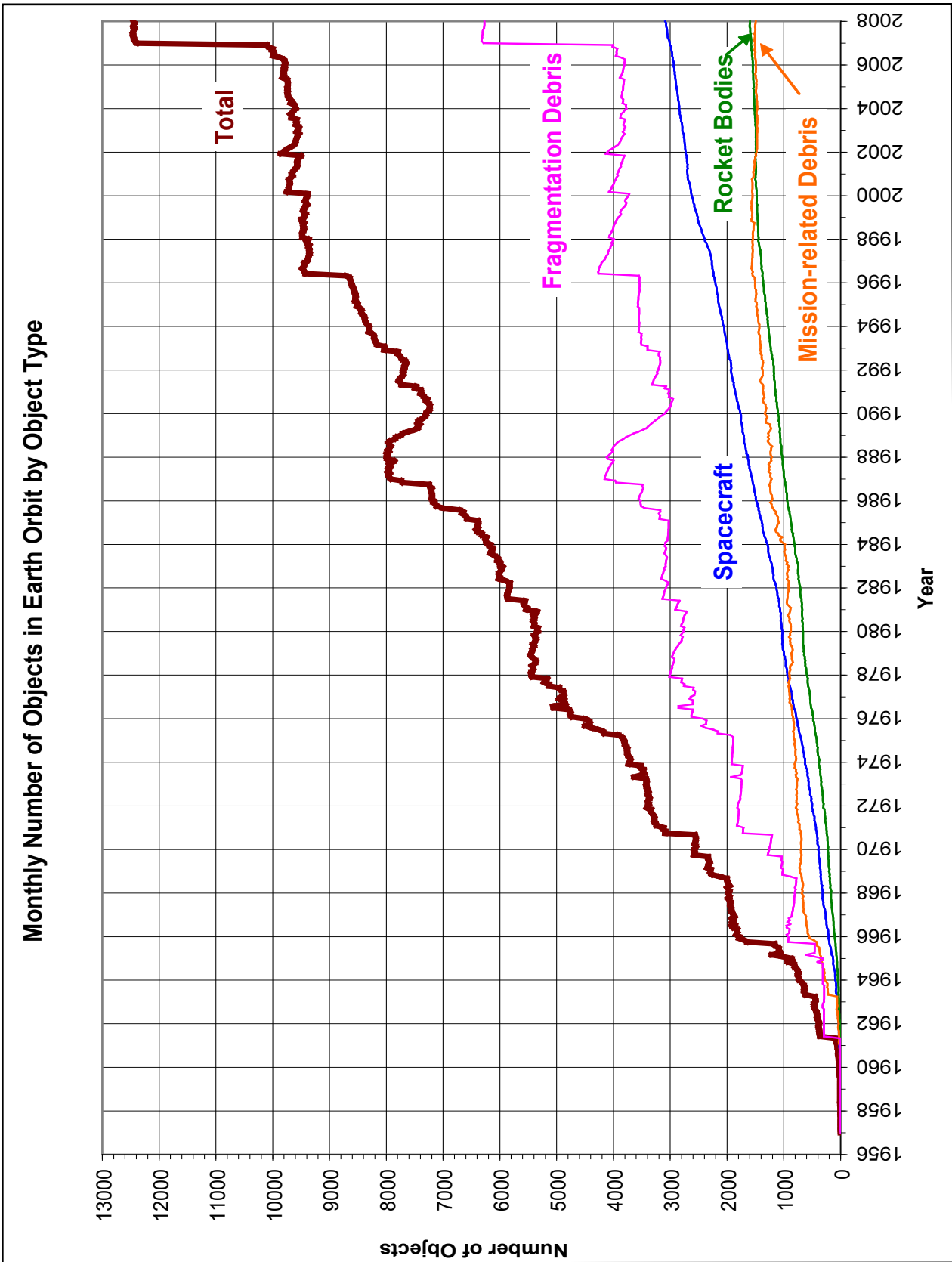
Monthly Number of Cataloged Objects in Earth Orbit by Object Type: This chart displays a summary of all objects in Earth orbit officially cataloged by the U.S. Space Surveillance Network. "Fragmentation debris" includes satellite breakup debris and anomalous event debris, while "mission-related debris" includes all objects dispensed, separated, or released as part of the planned mission.

National Aeronautics and Space Administration

Lyndon B. Johnson Space Center
2101 NASA Parkway
Houston, TX 77058

www.nasa.gov